Journal of Alloys and Compounds, 183 (1992) 224–240
JALCOM 7034

A-axis-oriented $YBa_2Cu_3O_7/PrBa_2Cu_3O_7$ superlattices: growth and transport properties*

Jean-Marc Triscone†, Chang-Beom Eom, Yuri Suzuki and T. H. Geballe
Department of Applied Physics, Stanford University, Stanford CA 94305 (USA)

(Received July 1, 1991; accepted September 4, 1991)

Abstract

Recent results on the growth of *a*-axis-oriented $YBa_2Cu_3O_7/PrBa_2Cu_3O_7$ superlattices and their transport properties are reported. The films have extremely smooth surfaces and a high crystalline quality as revealed by X-ray, transmission electron microscopy and Rutherford-backscattering spectroscopy analysis. When a magnetic field is applied in the plane of the substrate, it is found that the resistive transitions of superlattices containing individual $YBa_2Cu_3O_7$ layers 24 or 48 Å thick separated by $PrBa_2Cu_3O_7$ layers 24 or 48 Å thick show a cross-over at a temperature T^* which depends on the $PrBa_2Cu_3O_7$ thickness; above T^* the transition is insensitive to magnetic fields up to 8 T; below T^* some broadening occurs. These results are related to an abrupt disappearance of the coupling between the $YBa_2Cu_3O_7$ channels in the structure above T^*.

1. Introduction

High T_c superconductors (HTSs) are characterized by a layered anisotropic structure containing CuO_2 planes. This natural anisotropy reflects itself in many transport properties and is one of the key features of these materials. The anisotropic properties can be observed directly by using either single crystals or epitaxial thin films. Recently several groups succeeded in growing HTS superlattices [1–8]. These structures are of great interest since they offer the possibility to modify in a systematic way some intrinsic material properties such as the anisotropy. These studies are motivated by the need for key experiments to understand the effect of the nearly two-dimensional nature of these materials on the high critical temperature itself as well as on some of the particular and complex properties of HTSs. In the "123" family the *c*-axis-oriented $YBa_2Cu_3O_7/PrBa_2Cu_3O_7$ (YBCO/PBCO) multilayer system has been the most studied [2–4]; the effect of changing the distance between ultrathin YBCO layers by progressively inserting thicker insulating PBCO layers has been specially investigated. These multilayers also proved themselves to be an efficient model system to study flux motion in HTSs

*Dedicated to Professor W. Bronger and Professor Ch. J. Raub on the occasions of their 60th birthdays.

†On leave from Condensed Matter Department, University of Geneva, 24 Quai E.-Ansermet, CH-1211 Geneva 4, Switzerland.

0925-8388/92/$5.00

[9, 10]. One of the findings is that very thin layers of PBCO, typically 24–48 Å, are sufficient to suppress the Josephson coupling between the YBCO layers [10]. This small decoupling length is partly related to the short superconducting coherence length in the *c* direction since the coupling has to occur, by construction, in the *c* axis direction. From this point of view *a*-axis-oriented multilayers are very attractive since tunneling or proximity effects will make use of the longer *ab* superconducting coherence length. This last point is a key requirement for technological applications such as Josephson junctions; *a*-axis YBCO/PBCO heterostructures are certainly very attractive candidates for such realizations, although PBCO is not an ideal insulator [11].

We recently reported the successful growth of *a*-axis-oriented YBCO/PBCO superlattices with modulation wavelength Λ down to 24 Å [12]. Figure 1 is a schematic diagram of an *a* axis 12 Å/12 Å multilayer. The main thing to note is that unlike *c* axis multilayers [1–4], these structures have the CuO_2 planes perpendicular to the substrate surface. The artificial modulation takes place on lattice sites in the plane between the two CuO_2 planes. The situation is very different in *c* axis YBCO/PBCO multilayers where, ideally, each group of CuO_2 planes is either superconducting or insulating depending on whether the inner plane is yttrium or praseodymium. In *a* axis multilayers each CuO_2 plane has both types of neighbors. Apart from the above-mentioned technological interest in such structures, these YBCO/PBCO superlattices raise the following interesting question: will this structure display a kind of average behavior or comport itself as anticipated in Fig. 1, *i.e.* in alternating superconducting and insulating channels whose widths are determined by the rare earth modulation in the adjacent plane? In the latter case this system should, by changing the YBCO thickness, go from an essentially 2D coupled

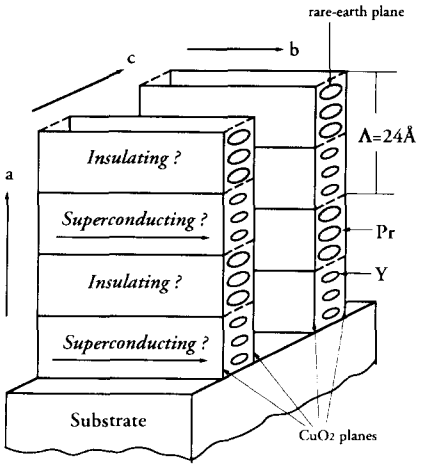

Fig. 1. Schematic diagram of an ideal 12 Å/12 Å *a* axis YBCO/PBCO superlattice. Note that the CuO_2 planes are vertical and that the rare earth modulation shown by the different-sized ellipsoids takes place between the two CuO_2 planes.

system for thick YBCO layers to a 1D coupled system for YBCO thicknesses smaller than the *ab* superconducting coherence length. Furthermore, for a given YBCO thickness one should be able to observe a cross-over from 1*D* to 2*D* coupling if, as one reduces the temperature, the superconducting coherence length decreases from greater than the channel width close to T_c to smaller. These multilayers also give us the opportunity to study the coupling between YBCO layers through *a* axis PBCO and thus to extract the coupling length, which is of great importance for any device construction and subject to an existing controversy*.

In this paper we review our recent findings on the growth and superconducting properties of these superlattices. We especially extend our analysis of the behavior of the resistive transitions in a magnetic field which demonstrate that these structures behave effectively as insulating–superconducting channels. The effect of the magnetic field on the resistive transition has been the subject of a short report [14].

We are pleased with the opportunity to publish this work in an issue dedicated to Dr. Chris Raub. One of us (T.H.G.) remembers his generosity and expertise in the laboratory and the excitement shared with him, Professor (then graduate student) Al Sweedler and Professor Bernd Matthias upon the discovery of superconductivity in the tungsten bronzes [15]. At that time we were puzzled by the fact that the superconductivity was found in the non-cubic perovskite, a violation of the empirical wisdom that cubic structures favored superconductivity. Actually, anisotropy turns out to be an important and perhaps essential aspect of the high T_c cuprates which this paper explores in the extreme.

2. Preparation and characterization

The superlattices were prepared using a 90° off-axis single-target sputtering technique which has been introduced at Stanford and described in detail in ref. 16. A schematic diagram of the system is shown in Fig. 2. Figure 2(a) shows the 90° off-axis sputtering geometry and Fig. 2(b) the configuration used for the multilayer growth where two sputter guns are oriented perpendicularly to each other. The substrate block is placed on a rotating arm to switch between guns. A computer-controlled stepping motor sets the dwell time at each gun, the acceleration and the velocity of the substrate block. The substrates used for the *a* axis growth were (100)$SrTiO_3$, (100)$LaAlO_3$ and (100)MgO with a (100)$SrTiO_3$ buffer layer. The sputtering atmosphere consisted of 40 mTorr O_2 and 60 mTorr Ar. The r.f. power (125 W) on the YBCO and PBCO sputter guns generated a self-bias of -50 and -150 V respectively. The substrate block temperature was held at 640 °C.

*Large coherence lengths for PBCO as well as for other insulating perovskites have been reported by Barner *et al.* and Tarutani *et al.* [13] in contradiction to the findings of Lew *et al.* [11].

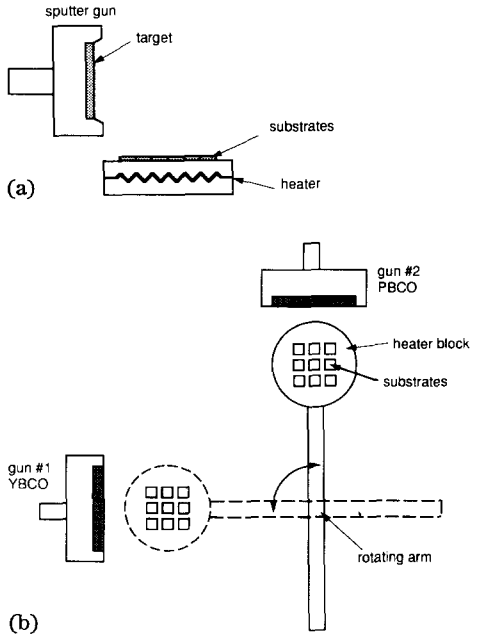

Fig. 2. Schematic configurations of (a) the 90° off-axis sputtering technique and (b) the system used to prepare the multilayers.

To obtain an *a* axis growth, one has to reduce the surface mobility; thus the substrate temperature along with the O_2 partial pressure are the important parameters to control. The deposition rates of YBCO and PBCO under these conditions were 0.2 and 0.6 Å s^{-1} respectively. The system configuration has been designed to facilitate the formation of sharp YBCO–PBCO interfaces during the switching between guns. The films studied here were prepared on (100)$LaAlO_3$ and had total film thicknesses between 2400 and 4800 Å. The initial reports on the successful growth and on the characterization of *a* axis single layers and of these *a* axis superlattices can be found in refs. 17 and 12 respectively.

An important feature of this 90° off-axis preparation technique is the surface smoothness, which is an essential requirement for the realization of heterostructures. Our films have surfaces with no detectable features in high resolution scanning electron microscope photographs (resolution approximately 100 Å). Using a scanning force microscope, we measured a 40 Å maximum feature height over a 16 μm^2 area.

In *a*-axis-oriented multilayers the interdiffusion between yttrium and praseodymium seems *a priori* to be more probable than in *c* axis multilayers since each rare earth plane contains both yttrium and praseodymium. We therefore carried a careful characterization of the films using X-ray diffraction, transmission electron microscopy (TEM) and Rutherford-backscattering spectroscopy (RBS). TEM, X-ray and ion channeling all show that the interfaces in the multilayered structure introduce no degradation of the overall crystalline

quality [12]. The X-ray FWHM (full width at half-maximum) of the main peaks and satellites was 0.06° and the ratio of the backscattered yield along ⟨100⟩ to that in a random direction (χ_{min}) is 3%, which is very close to the value of single crystals [18]. TEM and X-ray analysis show that we obtained a modulated structure down to a modulation wavelength Λ of 24 Å, suggesting a weak interdiffusion also in this growth orientation. Our evidence indicates that the conditions under which *a* axis films grow (*e.g.* the fact that each plane perpendicular to the growth direction contains all three cations) lead to films with fewer defects, *e.g.* antisite disorders, than *c* axis films.

Figure 3 is a cross-sectional transmission electron microscopy image of a YBCO/PBCO *a* axis superlattice. Figure 3(a) is a bright field image of the multilayer taken with no diffraction spots strongly excited. The principal contrast, corresponding to the composition modulation, is due to the difference in atomic number between praseodymium and yttrium. The superlattice period was found to be 21 Å, a value confirmed by X-ray analysis. Figure 3 illustrates the following interesting point: since the wavelength is not a multiple of the *a* axis lattice parameter, the interface layers necessarily contain a YPr solid solution. This particular sample is an extreme case; in general we precisely monitor the rates in order to switch as closely as possible to the completion of an atomic layer. Our X-ray studies [12] have demonstrated that we are able to control the wavelength of the multilayers within the experimental error of its determination via X-ray satellite peak positions. Therefore the multilayers studied here should have a limited mixing at the interfaces. This interface mixing problem, which always arises since the calibrations are never 100% perfect, generates a drift of the interface composition as a function of its position throughout the structure. Depending on the individual and total thicknesses, several layers with nearly ideal interfaces and thus optimum superconducting properties will be found in the multilayer. If the current

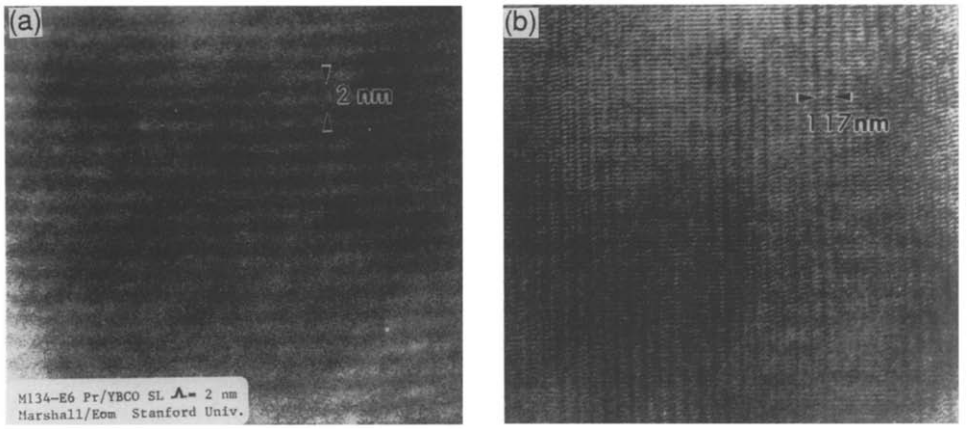

Fig. 3. Cross-sectional TEM images of an *a* axis $\Lambda = 21$ Å YBCO/PBCO superlattice prepared on (100)$SrTiO_3$: (a) with the specimen tilted away from a major zone axis to get the mass thickness contrast; (b) a high resolution image on the [010] zone axis (after ref. 12).

density is not too large, one should in principle probe the superconducting properties of these particular layers. For short periods the interface mixing problem is most important because the YBCO-side interface is a substantial fraction of the conduction path. Additionally, for thin periods when the switching occurs far from the completion of an atomic plane, any ideal layer in the multilayer will have a neighbor YBCO layer with non-optimum interface and thus depleted superconducting properties, rendering the coupling between these layers difficult. These points illustrate why it is important to switch as closely as possible to the completion of an atomic plane. The fact that we did not observe any detectable change in our measurements when changing the current density leads us to believe that this problem is not relevant for our samples.

In Fig. 3(a) the layers appear well separated, straight and continuous. Close examination of this sample, and also of a $\Lambda = 70$ Å sample, shows that typically the modulations in adjacent grains are in phase. In both samples curvature of the modulation is apparent on a larger scale than that shown in Fig. 3(a), but this curvature does not tend to disrupt the continuity of the modulation across grain boundaries. Figure 3(b) is a lattice image taken on a zone axis. Here the composition modulation contrast is obscured but the lattice quality is more apparent. The lattice fringes, both perpendicular and parallel to the layers, are imaged and indicate a high degree of crystalline perfection through the multilayers. These fringes remain straight throughout the structure. An important point (not visible on Fig. 3) is that although these films are untwinned, they still contain two types of grains which result from the growth on a cubic substrate. These grains represent domains with a 90° rotation of the *c* axis which strongly affect the transport properties. Typically the size of these *bc* and *cb* grains is 100–1000 Å. The J_cs of these films were measured at 4.2 K from magnetization hysteresis loops using Bean's methodology. The magnitude of about 1×10^6 A cm^{-2} was only slightly dependent upon the applied field [17], indicating that the grains do not exhibit weak link Josephson behavior. Furthermore, only a weak dependence upon the orientation of H in the plane is found with respect to the grain boundaries (see discussion of Fig. 7 below).

3. Transport properties

Figure 4, taken from ref. 12, shows resistivity *vs.* temperature curves for a $Y_{0.5}Pr_{0.5}BCO$ alloy *a* axis thin film and for 12/12 and 24 Å/24 Å *a* axis YBCO/PBCO superlattices. The alloy was made by a 2 Å YBCO/2 Å PBCO modulation. All the samples were photolitographically patterned (400 μm wide bridge) and the resistivity measurements were standard four-point measurements. First note that the resistivity values are much higher than in *c* axis materials, presumably owing to the numerous grain boundaries present in the *a* axis films and to the longer effective path length which the current must follow in order to flow in the high conductivity *ab* planes [12,

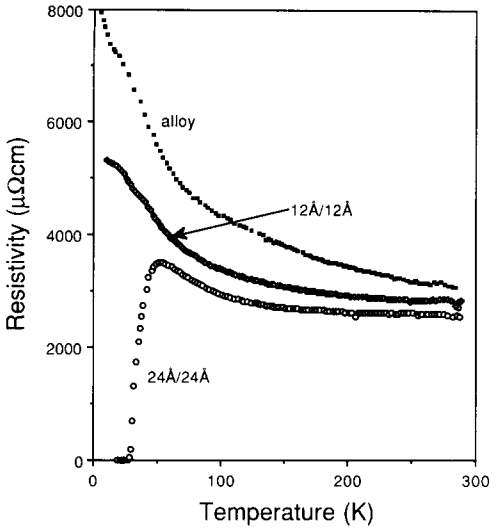

Fig. 4. Resistivity *vs.* temperature curves for a $Y_{0.5}Pr_{0.5}BCO$ alloy *a* axis film and for 12/12 and 24 Å/24 Å *a* axis YBCO/PBCO superlattices.

17]. There are also striking differences between the superconducting properties of *a* axis and *c* axis superlattices: the T_{c0} of the 24 Å/24 Å *a* axis multilayer is 30 K, compared with 70 K for a similar wavelength *c* axis multilayer grown at 720 °C [2–4], and for 12 Å/12 Å multilayers a *c* axis multilayer prepared on MgO under non-optimal conditions for *c* axis growth, at the same time as the *a* axis multilayers were being deposited, had a T_{c0} of about 40 K, while the *a* axis films are not superconducting above 4.2 K. The possible explanations for these differences are discussed in ref. 12. We do not want here to review all these possibilities but note that the reason for the T_c depression of thin YBCO layers in *c* axis multilayers is still under debate. In the *a* axis multilayers at least two additional factors can play a role; first, the sheet resistance can be much greater than in *c* axis multilayers if the structure behaves as channels, since interface reflections within the CuO_2 planes are expected to lead to a sheet resistance for which localization effects may have to be considered; secondly, when the YBCO thickness is smaller than the *ab* zero-temperature superconducting coherence length (this is the case for 12 Å YBCO), one is in principle in a nearly 1D regime and 1D fluctuations may play a role. For such thin YBCO layers the Cooper pair wavefunction would have to extend into the PBCO layer, where the order parameter could be suppressed by the praseodymium magnetic moment, if, as still not yet established, the praseodymium is a pair-breaking scatterer.

As mentioned in Section 1, one of the interesting features of these multilayers is the possibility that they behave as insulating–superconducting channels whose widths depend on the PBCO and YBCO thicknesses respectively. To test these ideas, we measured the resistive transitions in a magnetic field for a single *a* axis YBCO film and for 24/24, 48/24 and 48

Å/48 Å *a* axis YBCO/PBCO multilayers. For these experiments it is important to consider the current–field configuration because of the two types of grains, *cb* and *bc*, which can be found in the films. Figure 5 shows the different measurement configurations we used. The films were patterned in 400 μm wide strips making a $\pm 45°$ angle with the *b* (or *c*) direction of both types of grains. The magnetic field was applied in the plane of the substrate either at a 45° angle to the macroscopic current, thus being parallel to half of the CuO_2 planes and perpendicular to the other half (configuration 1), or at a 90° angle to the macroscopic current, thus making a $\pm 45°$ angle with each CuO_2 plane (configuration 2). It was also applied perpendicular to the substrate surface, *i.e.* parallel to the CuO_2 planes (configuration 3). Configuration 2 ensures that each CuO_2 plane experiences the same perpendicular field (whose intensity is $1/2^{1/2}$ times the intensity of the applied field). To test whether the structures we were measuring were consistent with Fig. 5, we first measured an *a* axis single-layer YBCO film for different magnetic fields between 0 and 8 T with configuration 2. The result is shown in Fig. 6. One sees that below 1 T the broadening is close, as expected, to what is observed for *c* axis films with the field applied parallel to the *c* axis (see *e.g.* ref. 19). Surprisingly, above 1 T the curves are described simply by a shift of the transition with only a small additional broadening. If one tries to extract an upper critical field from these data assuming that only the perpendicular field gives a significant contribution (thus we corrected the field intensity by $1/2^{1/2}$), we find for fields above 1 T that $H_{c2} \propto 1 - T/T_c$ with dH_{c2}/dT

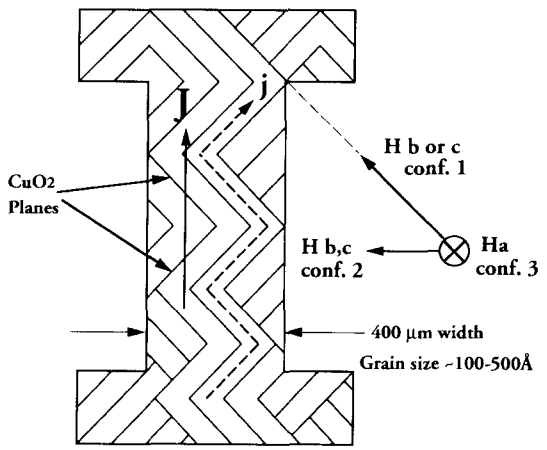

Fig. 5. A top view of the film after patterning showing the configuration measurement used for the resistive transitions in magnetic field. Because of the two types of grains, the films were patterned so that the macroscopic current makes a 45° angle with the CuO_2 planes (shown as the zigzag lines). The three different field configurations are shown. For configurations 1 and 2 the field is in the plane of the substrate. Configuration 1 has the field aligned with the CuO_2 planes of one type of grain, providing a parallel field for half of the CuO_2 planes and a perpendicular field for the other half. Configuration 2 provides a magnetic field making a 45° angle with each CuO_2 plane. For configuration 3 the field is perpendicular to the substrate plane and this corresponds to a magnetic field parallel to all *ab* planes.

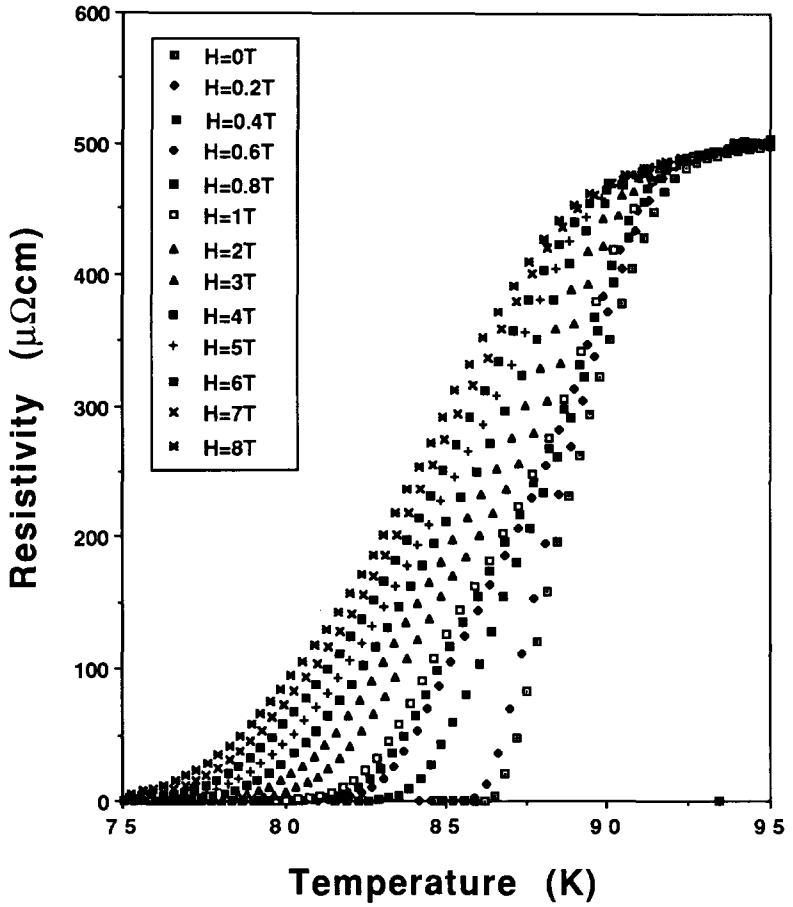

Fig. 6. Resistive transitions in magnetic field between 0 and 8 T for a single YBCO layer for configuration 2, *i.e.* each CuO_2 plane experiences a perpendicular field whose intensity is $1/2^{1/2}$ times the intensity of the applied field.

slopes ranging from -1.2 (10% criterion) to -2.6 T K^{-1} (90% criterion). These values do not show the wide spread observed in *c* axis materials depending on the choice of criterion [19] and are acceptably close to the -1.9 T perpendicular critical field slope obtained with magnetic measurements by Welp *et al.* [20]. This suggests that the finite thickness of the sample (2400 Å) may have reduced the flux-flow-induced broadening, perhaps in some way related to the deformation of the flux lattice which gives rise to the peak effects.

To check any unsuspected effect due to the field orientation, we rotated the field 45° in the plane of the substrate (configuration 1). Now, for half the current path the field is parallel to the CuO_2 planes and for the other half it is perpendicular. The planes which experience the parallel field will have a higher transition temperature than in the configuration 2 case where

the field is applied at a 45° angle and thus has a perpendicular component, while the planes which see the perpendicular field will have a lower transition temperature since now the perpendicular field is $2^{1/2}$ higher than in the other configuration. Comparing the curves for the two measurement configurations one expects these curves to cross at about 50% of the normal state resistance. This is exactly what we observe, as illustrated in Fig. 7 for a magnetic field of 3 T.

Let us turn now to the multilayers. Figure 8 shows the resistive transitions for a 24 Å/24 Å YBCO/PBCO multilayer for (a) configuration 2 with a current density of 100 A cm^{-2}, (b) configuration 2 but with a current density of 2 A cm^{-2} and (c) configuration 1 with a current density of 100 A cm^{-2}. In all cases there is a cross-over. Above a characteristic temperature T^* the structure is insensitive to the magnetic field; below T^* some broadening occurs. Rotating the field in the plane of the substrate does not change the insensitivity above T^* but produces for the bottom part of the transition

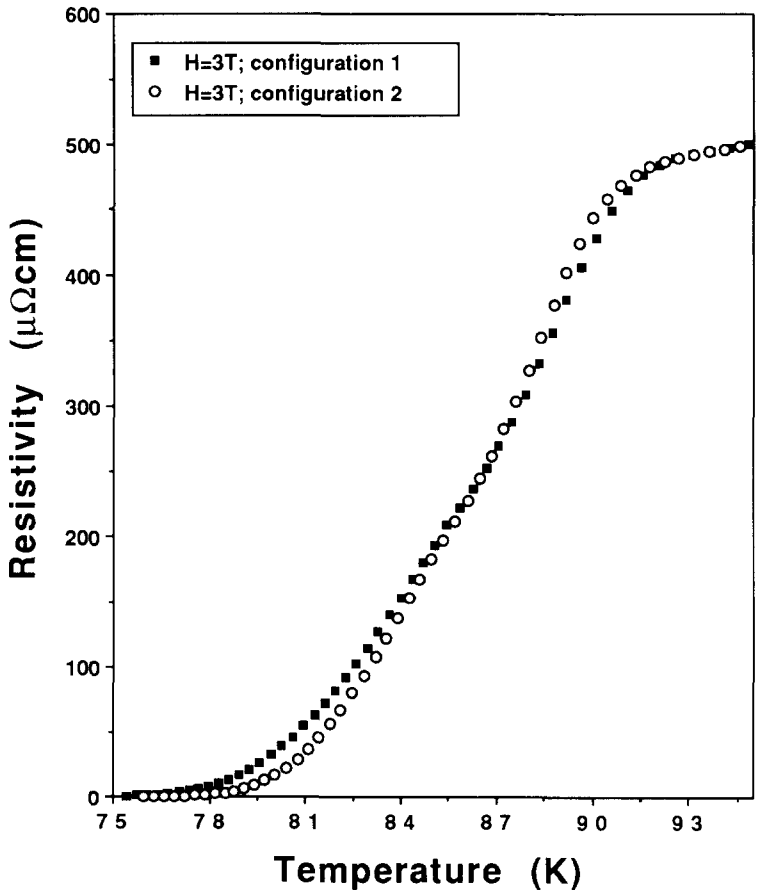

Fig. 7. Resistive transitions in a 3 T magnetic field for a single YBCO layer for configurations 1 and 2.

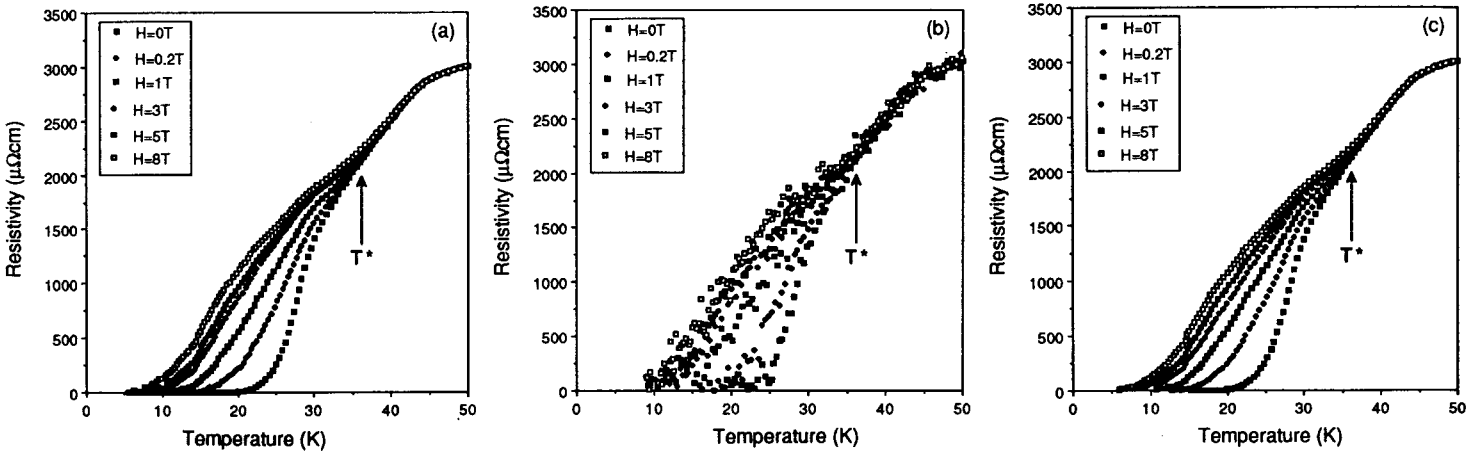

Fig. 8. Resistive transitions in magnetic field between 0 and 8 T for a 24 Å/24 Å multilayer with (a) configuration 2 and a current density of 100 A cm^{-2}, (b) configuration 2 and a current density of 2 A cm^{-2} and (c) configuration 1 and a current density of 100 A cm^{-2}.

the same effect as discussed above, *i.e.* a slightly larger broadening due to the higher perpendicular component of the field, although this effect is hard to see on the figure. Changing the current density by nearly two orders of magnitude (Fig. 8(b)) does not change the character of the data. T^* is not affected by this change, which means that this cross-over temperature is not Lorentz force related. T^* is thus current and field independent. This type of insensitivity has already been observed in c axis multilayers [21] and in very thin c axis films [22] but always for fields applied perpendicular to the c axis. In our case the field largely probes the wide broadening direction, *i.e.* field parallel to the c axis. We give here a simple explanation for this insensitivity. The very thin individual 24 Å YBCO layers cannot screen the magnetic field since they are much smaller than the penetration depth, so the magnetic field is nearly uniform in the structure. Now, if above T^* each YBCO channel is not coupled to the next, no screening current is able to flow from one channel to the next, each YBCO layer behaves independently and the material spends very little energy on screening. Additionally, such thin YBCO layers can have a very large H_{c1}. If one estimates H_{c1} in this field configuration for a thin superconducting film with the conditions $\xi < d < \lambda$, with ξ being the superconducting coherence length, d the film thickness and λ the penetration depth, one finds (see *e.g.* ref. 23) $H_{c1} = (2\phi_0/\pi d^2)\ \ln(d/\xi)$, where ϕ_0 is the flux quantum and $\xi \approx 15$ Å is the ab superconducting coherence length. A simple calculation shows that H_{c1} is above 105 and 65 T respectively for YBCO films 24 and 48 Å thick. Below these fields it is energetically unfavorable for the vortices to enter the layers. Thus without coupling between the layers (above T^*) there are no vortices in the YBCO layers and no dissipation associated with flux motion. If this explanation is correct, it implies that the parameter which determines T^* is the PBCO thickness since this thickness controls the coupling between the YBCO layers. We checked this by making a 48 Å YBCO/24 Å PBCO multilayer. Although T_c is slightly higher, the result is essentially the same as that shown in Fig. 8, *i.e.* the decoupling takes place at about 70% of the normal state resistivity. If one increases the PBCO thickness, one expects to get more decoupled YBCO layers. The result for a 48 Å/48 Å multilayer is shown in Fig. 9 (configuration 2). We find that an 8 T field does not produce any effect on most of the resistive transition. Within our measurement accuracy, about 0.15 K, we do not observe any shift or broadening for $\rho \gtrsim 20\% \rho(100\ \text{K})$.

In the tail of the transition some broadening occurs which is much more evident in Fig. 10, where the data are plotted in an Arrhenius manner, *i.e.* log ρ *vs.* $1/T$. This kind of plot is used to illustrate a thermally activated behavior. In high T_c crystals and for $\rho \ll \rho_n$ the observed activated behavior is understood as a result of thermally activated flux flow (TAFF) [24, 25]. What we observe in Fig. 10 for our samples is that the low resistivity part of the transition display an approximately linear behavior corresponding to activation energies ranging from about 1400 K in zero field to about 300 K at 8 T, values much smaller than for pure YBCO. These numbers have to be taken with care since we do not know the exact temperature dependence

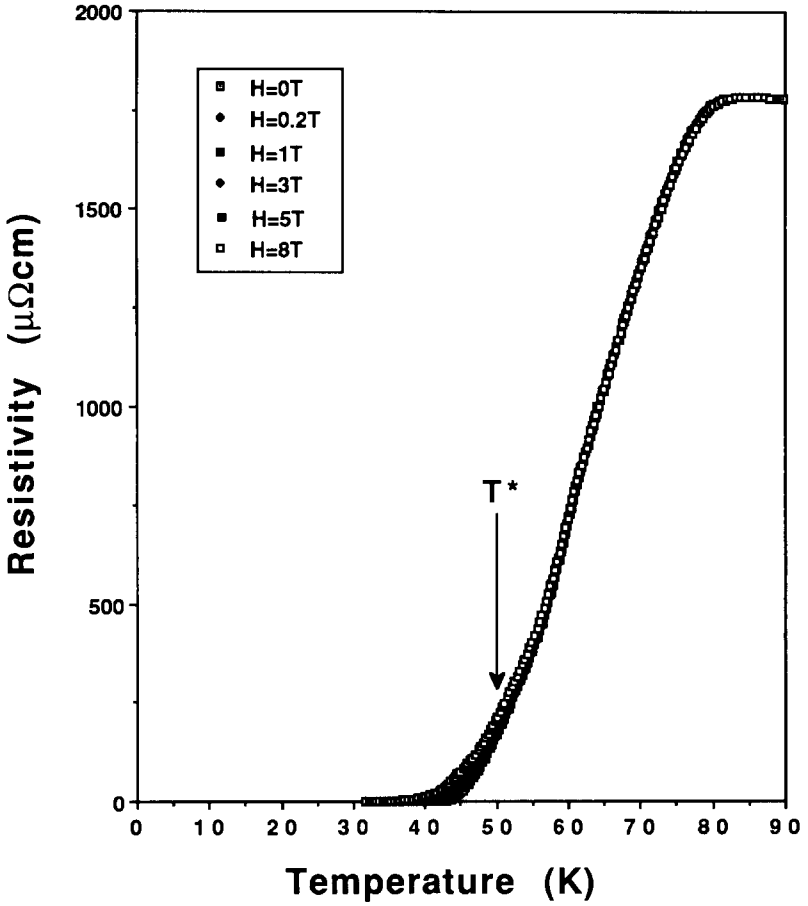

Fig. 9. Resistive transitions in magnetic field between 0 and 8 T for a 48 Å/48 Å multilayer with configuration 2, *i.e.* each CuO_2 plane experiences a perpendicular field.

of the activation energy. The fact that these curves are very close to straight lines, however, suggests that the activation energy U has a temperature dependence close to $U=U(T=0)(1-T/T_c)$ and in this case the slope of the Arrhenius plot gives a value near the zero-temperature activation energy. If what we observe is effectively the signature of TAFF, it can be taken as an evidence that below T^*, because of the coupling across PBCO, some vortices are present in the structure and the dissipation is related to their motion. We also observed a break in the curves at $T'=44$ K ($1/T'=0.023$), which is the bottom of the transition (see Fig. 9). This may be the signature of a change in the dissipation process, possibly from thermally activated flux flow at low temperatures to flux flow between T' and T^*.

By comparing Figs. 8 and 9, one sees that increasing the PBCO thickness effectively produces a stronger decoupling of the YBCO channels. The implication of these results is that in the insensitive part of the transition

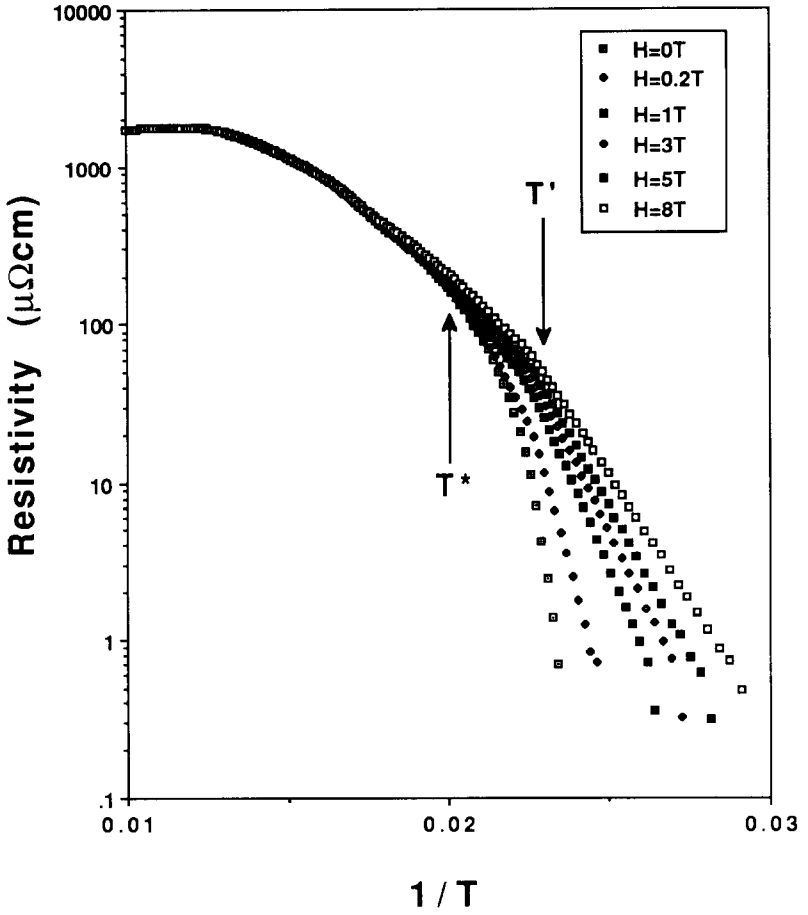

Fig. 10. Arrhenius plot of the resistive transitions in magnetic field between 0 and 8 T for a 48 Å/48 Å multilayer with configuration 2.

the current is not flowing from one YBCO channel to the next. This is a very striking result since it implies that the structure behaves as shown in Fig. 1, *i.e.* as insulating–superconducting channels. The decoupling at high temperature may be due to thermal fluctuations in the PBCO layers suppressing the Josephson coupling. These results have also some implications on the nature of the suppression of superconductivity in pure PBCO since the Pr^{4+} electron-doping model should lead to an averaging-out in the multilayers. In other words it is hard to understand the insulating–superconducting channels within this picture since it would imply that the additional electrons injected are "localized" in the PBCO channels. Other explanations for the T_c reduction such as a depression due to the magnetic moment of praseodymium are compatible with our experimental results.

What do we learn about the coupling through *a* axis PBCO? Although more samples are necessary to find the PBCO decoupling length, comparison

with the c axis results shows that the decoupling produced by 12 and 24 Å c axis PBCO in c axis YBCO/PBCO multilayers [21] roughly resembles the decoupling produced respectively by 24 and 48 Å a axis PBCO in a axis YBCO/PBCO multilayers. This suggests that the a axis PBCO thickness necessary to completely decouple YBCO layers is twice the c axis value or about 100 Å.

Finally we discuss the results in fields parallel to the CuO_2 planes (configuration 3). For the a axis single YBCO layer the broadening is less than that obtained for configuration 2 (Fig. 6) as expected, because with a parallel field we probe the low broadening, high critical field orientation. However, for all the multilayers studied here we find that the broadening is larger for this latter field orientation. This is illustrated in Fig. 11 for the 48 Å/48 Å multilayer. As one sees, the broadening is clearly more important than that in Fig. 9 and this is still true for the bottom part of the transition

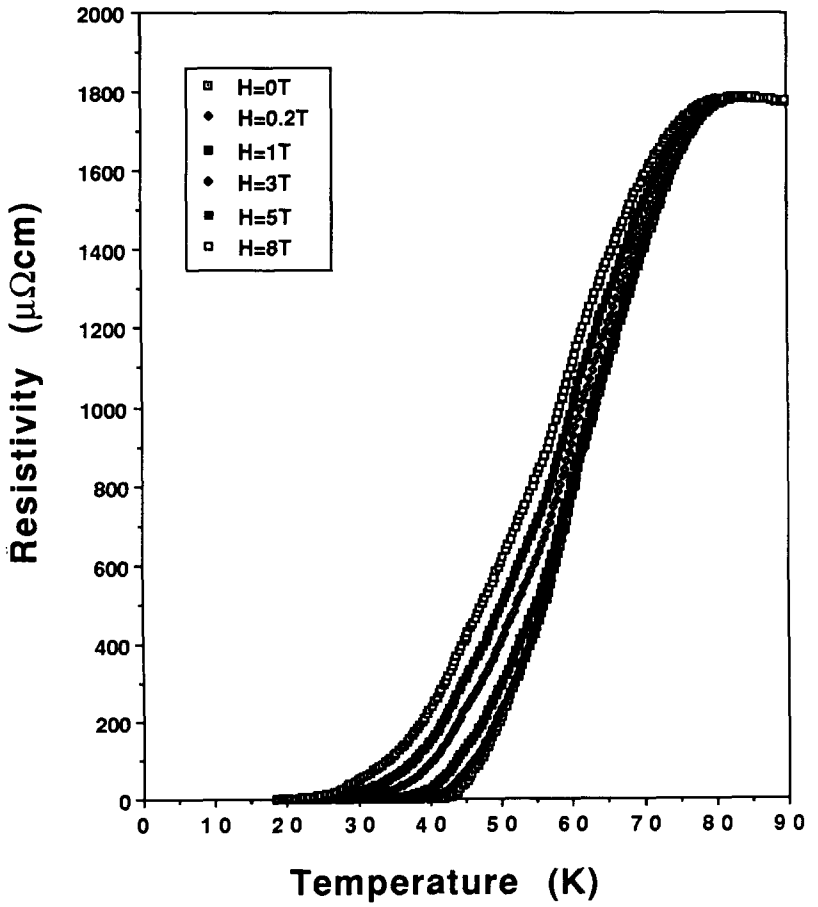

Fig. 11. Resistive transitions in magnetic field between 0 and 8 T for a 48 Å/48 Å multilayer with configuration 3, *i.e.* each CuO_2 plane experiences only a parallel field.

for all the multilayers where the curves are sensitive to the magnetic field. This leads to a lower activation energy for this latter field orientation which may be related to the fact that the activated volume (and thus the activation energy) has been cut by the artificial layering as has been demonstrated to be the case in c axis superlattices*. More data are necessary to clarify this last point.

4. Conclusions

We have studied a-axis-oriented $YBa_2Cu_3O_7/PrBa_2Cu_3O_7$ superlattices grown using a 90° off-axis sputtering technique. The film surfaces are extremely smooth and the crystalline quality of the superlattices, examined by X-ray, TEM and RBS, is excellent. The X-ray FWHM of the main and satellites reflections is only 0.06° and the RBS ratio of the backscattered yield along $\langle 100 \rangle$ to that in a random direction (χ_{min}) is 3%. When a magnetic field is applied in the plane of the substrate, we find that the resistive transitions of superlattices with modulation wavelengths of 96 Å (48 Å $YBa_2Cu_3O_7$/48 Å $PrBa_2Cu_3O_7$), 72 Å (48 Å $YBa_2Cu_3O_7$/24 Å $PrBa_2Cu_3O_7$) and 48 Å (24 Å $YBa_2Cu_3O_7$/24 Å $PrBa_2Cu_3O_7$) show a cross-over with the upper part of the transition insensitive to magnetic fields up to 8 T. The cross-over temperature is controlled by the PBCO thickness. These results show that in the temperature range where we observe this insensitivity the structure behaves as superconducting–insulating channels whose width is determined by the $YBa_2Cu_3O_7$ and $PrBa_2Cu_3O_7$ thicknesses. By comparing these results with what is obtained on c axis superlattices, we estimated that 100 Å a axis PBCO should produce complete decoupling of the YBCO channels. The channel dimensions and the perfection of the superlattices are such that the study of quasi-1D transport is feasible.

Acknowledgments

We would like to thank Mac Beasley and Seb Doniach for helpful discussions on the implications of the experiment, Steve Laderman for sharing his expertise of X-ray diffraction and Ann Marshall for the TEM analysis. This work was supported by the Air Force Office for Scientific Research under contract F49629-89-C-001, by the Stanford Center for Materials Research under the NSF–MRL program and by the Electrical Power Research Institute. One of us (J.-M.T.) would like to thank the "Fonds National Suisse de la Recherche Scientifique" for giving him the opportunity to be at Stanford University for the past year.

*The activation energy can be written [23] as $U \propto H_c^2 V_c$, where V_c is the volume involved in a flux jump. $V_c = AL_c$, where A is a correlation area in the plane and L_c is a correlation length along the vortex line. If L_c(YBCO) is larger than the individual YBCO layer thickness in the multilayer, L_c will be restricted by construction, thus reducing V_c and U [9, 10].

References

1 J.-M. Triscone, M. G. Karkut, L. Antognazza, O. Brunner and Ø. Fischer, *Phys. Rev. Lett.*, *63* (1989) 1016.
2 J.-M. Triscone, Ø. Fischer, O. Brunner, L. Antognazza, A. D. Kent and M. G. Karkut, *Phys. Rev. Lett.*, *64* (1990) 804.
3 Q. Li, X. X. Xi, X. D. Wu, A. Inam, S. Vadlamannati, W. L. McLean, T. Venkatesan, R. Ramesh, D. M. Hwang, J. A. Martinez and L. Nazar, *Phys. Rev. Lett.*, *64* (1990) 3086.
4 D. H. Lowndes, D. P. Norton and J. D. Budai, *Phys. Rev. Lett.*, *65* (1990) 1160.
5 A. Gupta, R. Gross, E. Olsson, A. Segmüller, G. Koren and C. C. Tsuei, *Phys. Rev. Lett.*, *64* (1990) 3191.
6 T. Matsushima, Y. Ichikawa, H. Adachi, K. Setsune and K. Wasa, *Solid State Commun.*, *76* (1990) 1201.
7 M. Kanai, T. Kawai and S. Kawai, *Appl. Phys. Lett.*, *57* (1990) 198.
8 I. Bozovic, J. N. Eckstein, M. E. Klausmeier-Brown and G. Virshup, *J. Superconductivity*, in the press.
9 O. Brunner, L. Antognazza, J.-M. Triscone, L. Miéville and Ø. Fischer, *Phys. Rev. Lett.*, *67* (1991) 1354.
10 J.-M. Triscone, L. Antognazza, O. Brunner, L. Miéville, M. G. Karkut, O. Eibl, P. van der Linden, J. A. A. J. Perenboom and Ø. Fischer, *Physica C*, *185–189* (1991) 210.
11 D. Lew, Y. Suzuki, C. B. Eom, M. Lee, J.-M. Triscone, T. H. Geballe and M. R. Beasley, *Physica C*, *185–189* (1991) 2553.
12 C. B. Eom, A. F. Marshall, J.-M. Triscone, S. S. Laderman, B. Wilkens and T. H. Geballe, *Science*, *251* (1991) 780.
13 J. B. Barner, C. T. Rogers, A. Inam, R. Ramesh and S. Bersey, *Appl. Phys. Lett.*, *59* (1991) 742.
Y. Tarutani, T. Fukazawa, U. Kabasawa, A. Tsukamoto, M. Hiratani, M. Suga and K. Takagi, *Proc. 3rd FED Workshop, Kumamoto, May 1991*, in press.
14 C. B. Eom, J.-M. Triscone, Y. Suzuki and T. H. Geballe, *Physica C*, *185–189* (1991) 2065.
15 A. R. Sweedler, Ch. J. Raub and B. T. Matthias, *Phys. Lett.*, *15* (1965) 108.
16 C. B. Eom, J. Z. Sun, B. M. Lairson, S. K. Streiffer, A. F. Marshall, K. Yamamoto, S. M. Anlage, J. C. Bravman, T. H. Geballe, S. S. Laderman, R. C. Taber and R. D. Jacowitz, *Physica C*, *171* (1990) 354.
17 C. B. Eom, A. F. Marshall, S. S. Laderman, R. D. Jacowitz and T. H. Geballe, *Science*, *249* (1990) 1549.
18 N. G. Stoffel, P. A. Morris, W. A. Bonner and B. J. Wilkens, *Phys. Rev. B*, *37* (1988) 2297.
19 Y. Iye, T. Tamegai, T. Sakakibara, T. Goto, N. Miura, H. Takeya and H. Takai, *Physica C*, *153–155* (1988) 26.
20 U. Welp, W. K. Kwok, G. W. Crabtree, K. G. Vandervoort and J. Z. Liu, *Phys. Rev. Lett.*, *62* (1989) 1908.
21 O. Brunner, J.-M. Triscone, L. Antognazza, M. G. Karkut and Ø. Fischer, *Physica B*, *165–166* (1990) 469.
22 T. Terashima, K. Shimura, Y. Bando, Y. Matsuda, A. Fujiyama and S. Komiyama, *Phys. Rev. Lett.*, *67* (1991) 1362.
23 T. P. Orlando and K. A. Delin, *Foundations of Superconductivity*, Addison-Wesley, Reading, MA, 1991, p. 388.
24 T. T. M. Palstra, B. Batlogg, R. B. van Dover, L. F. Schneemeyer and J. V. Waszczak, *Phys. Rev. B*, *41* (1990) 6621.
25 T. T. M. Palstra, B. Batlogg, L. F. Schneemeyer and J. V. Waszczak, *Phys. Rev. B*, *43* (1991) 3756.